Brain (2002), **125,** 1558–1569

Dopamine-dependent changes in the functional connectivity between basal ganglia and cerebral cortex in humans

David Williams,[1] Marina Tijssen,[2] Gerard van Bruggen,[2] Andries Bosch,[3] Angelo Insola,[4] Vincenzo Di Lazzaro,[5] Paolo Mazzone,[4] Antonio Oliviero,[5] Angelo Quartarone,[6] Hans Speelman[3] and Peter Brown[1]

[1]*Sobell Department of Neurophysiology, Institute of Neurology, London, UK,* [2]*Department of Neurology and* [3]*Department of Neurosurgery, Academic Medical Centre, Amsterdam, The Netherlands,* [4]*Operative Unit of Functional and Stereotactic Neurosurgery CTO 'A. Alesini' Hospital,* [5]*Institute of Neurology, Università Cattolica, Rome and* [6]*Institute of Neurological and Neurosurgical Sciences, University of Messina, Messina, Sicily, Italy*

Correspondence to: P. Brown, Sobell Department of Neurophysiology, Institute of Neurology, Queen Square, London WCIN 3BG, UK
E-mail: p.brown@ion.ac.uk

Summary

We test the hypothesis that interaction between the human basal ganglia and cerebral cortex involves activity in multiple functional circuits characterized by their frequency of oscillation, phase characteristics, dopamine dependency and topography. To this end we took recordings from macroelectrodes (MEs) inserted into the subthalamic nucleus (STN) in eight awake patients following functional neurosurgery for Parkinson's disease. An EEG was also recorded, as were the signals from MEs in the globus pallidus interna (GPi) in two of the cases. Coherence between EEG and ME potentials was apparent in three major frequency bands, 2–10 Hz, 10–30 Hz and 70–85 Hz. These rhythmic activities differed in their cortical topography, although coherence was always strongest over the midline. Coherence between EEG and ME potentials in the 70–85 Hz band was only recorded in patients treated with levodopa. Cortical activity phase led that in the basal ganglia in those oscillatory activities with frequencies <30 Hz. In contrast, STN and GPi phase led cortex in the 70–85 Hz band. The temporal differences in the way in which cortical activity led or lagged behind that in STN/GPi were similar, around 20 ms, regardless of the overall direction of information flow and frequency band. We conclude that the basal ganglia may receive multiple cortical inputs at frequencies <30 Hz and, in the presence of dopaminergic activity, produce a high frequency drive back to the cerebral cortex, in particular the supplementary motor area (SMA).

Keywords: coherence; deep brain stimulation; motor cortex; Parkinson's disease; subthalamic nucleus

Abbreviations: CL = confidence limit; GPi = globus pallidus interna; LP = local potential; ME = macroelectrode; SMA = supplementary motor area; STN = subthalamic nucleus

Introduction

The nature of subcortico–cortical interactions within the motor system has been difficult to establish in humans, partly due to the inaccessibility of the basal ganglia and cerebellum to neurophysiological investigation. The recent resurgence of interest in deep brain electrode implantation and stimulation as a treatment for movement disorders has offered the unique opportunity to record from the cerebellar thalamus (Marsden *et al*., 2000) and basal ganglia in alert and cooperative patients. We recently showed that activity in the human subthalamic nucleus (STN) was synchronized with that in the globus pallidus interna (GPi) and tended to be oscillatory in nature (Brown *et al*., 2001). Oscillations occurred in two broad bands: <30 Hz and 70–85 Hz. Oscillatory coupling in the

Table 1 *Clinical details and summary of coherence between STNME and EEG*

	Case*							
	1†	2†	3†	4†	5	6	7	8
Age (years) and sex	62 M	53 M	51 M	67 F	67 M	69 F	49 F	37 M
Disease duration (years)	16	9	11	28	13	15	17	10
Predominant symptom	Bradykinesia, rigidity	Tremor, dyskinesias	Response fluctuations	Response fluctuations, dyskinesias	Response fluctuations, dyskinesias	Bradykinesia, dyskinesias	Bradykinesia, dyskinesias	Bradykinesia, dyskinesias
Location of ME	Bilateral STN	Bilateral STN	Bilateral STN	Bilateral STN	R STN	Bilateral STN	L GPi and L STN	R GPi and R STN
Motor UPDRS on/off	37/50	21/31	14/48	27/53	10/69	10/69	12/80	7/65
Medication (daily dose)	Levodopa 600 mg, Pergolide 4 mg, Amantadine 300 mg	Levodopa 400 mg, Benzhexol 2 mg	Levodopa 500 mg, Selegiline 5 mg, Roperinole 20 mg, Entacapone 1000 mg	Levodopa 300 mg, Roperinole 5 mg	Levodopa 250 mg	Levodopa 1050 mg, Pramipexole 3 mg	Levodopa 1500 mg	Levodopa 150 mg, Ropinirole 4 mg
Coherence‡								
2–10 Hz	+	+	–	+	+	+	+	+
10–20 Hz	+	+	+	+	–	+	+	+
20–30 Hz	+	+	+	+	+	+	+	+
70–85 Hz	–	+	–	–	+	+	+	+

*Cases 2 and 4 were left handed.
†Simultaneous EEG recordings from several scalp sites possible.
‡Coherence between at least one STNME contact and at least one bipolar EEG lead >95% CL in two or more contiguous bins.
UPDRS = Unified Parkinson's Disease Rating Scale; R = right; L = left; M = male; F = female.

lower band was increased in parkinsonian patients withdrawn from levodopa and dopaminergic agonists, whereas that at ~70 Hz was seen only in treated patients. The lower frequency activity is not restricted to the STN–GP: loop and STN activity is coherent with that in the cerebral cortex in the same band, with cortex leading by ~20 ms (Marsden *et al*., 2001).

Here we investigate the cortical topography of the low frequency drive to STN, and determine whether the functional connectivity within the basal ganglia at ~70 Hz is also manifest in the coupling between STN and cerebral cortex. To this end we recorded local potentials (LPs) from subthalamic and GPi macroelectrodes (STNME and GPiME) following functional neurosurgery in eight cooperative, awake parkinsonian patients while simultaneously recording scalp EEG. In four of these patients, recordings were made following withdrawal and reinstitution of treatment with the dopamine precursor, levodopa, so as to investigate both low and high frequency coupling between cortex and basal ganglia. We show that the midline cortical areas hold a pre-eminent position in oscillatory coupling with the basal ganglia and that these cortical areas are driven by the STN at high frequency.

Methods

Patients and surgery

All patients participating in the study gave their informed consent, and their clinical details are summarized in Table 1. The operative procedure and beneficial clinical effects of stimulation have been described previously (Siegfried and Lippitz, 1994; Limousin *et al*., 1995; Starr *et al*., 1998; Volkmann *et al*., 1998). MEs were inserted after STN or GPi had been identified by ventriculography and preoperative MRI. Simultaneous implantation of bilateral STNME was performed in five cases, and of ipsilateral STNME and GPiME in two cases. In the latter, surgery was performed in the context of a comparative clinical study of the efficacy of stimulation at different sites at the Operative Unit of Functional and Stereotactic Neurosurgery CTO 'A. Alesini' Hospital, Rome. The intended coordinates at the tip of contact 0 were: 19–24 mm from the midline of the patient; 2 mm in front of the midcommissural point, 6 mm below the AC–PC (anterior commissure–posterior commissure) line for GPi and 12 mm from the midline; and 0–2 mm behind the midcommissural point and 4–5 mm below the AC–PC line for STN. Post-operative CT imaging or MRI (n = 2) was consistent with ME placement in the intended targets in Cases 5–8. The ME position determined by post-operative CT was

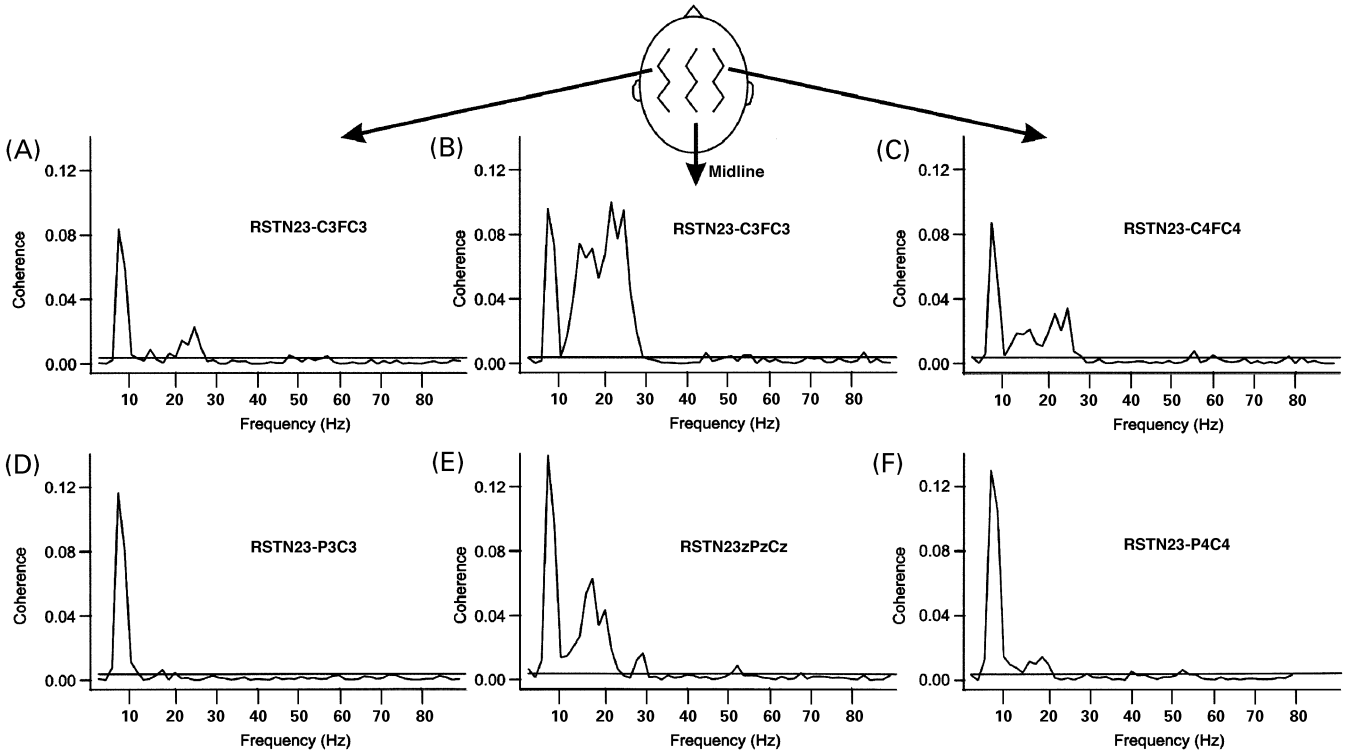

Fig. 1 Coherence spectra between the right (R) STNME23 and EEG in Case 1 on his usual anti-parkinsonian medication. Coherence is strongest over the midline (287 blocks have been averaged). The horizontal lines in the coherence spectra are the 95% CL. The apparent topographic difference in 2–10 and 20–30 Hz coherence was confirmed by two-way ANOVA (maximum mean coherences in 2–10 and 10–30 Hz bands, respectively, were 0.053, 0.045, 0.013, 0.020, and 0.056, 0.066, 0.067, 0.04 for the four subjects).

superimposed on pre-operative MRI using image fusion systems in two cases. No post-operative imaging was performed in Cases 1–4, on whom operations were performed at the Department of Neurosurgery, Academic Medical Centre, Amsterdam. The MEs in the pallidum and STN were models 3387 and 3389 (Medtronic Neurological Division, Minneapolis, MN, USA) with four platinum–iridium cylindrical surfaces (1.27 mm diameter, 1.5 mm length) and centre-to-centre separations of 3 and 2 mm, respectively. Contact 0 was the most caudal and contact 3 was the most rostral. Cases 1–4 were recorded on their usual anti-parkinsonian medication. Cases 5–8 were recorded after overnight withdrawal of anti-parkinsonian medication, and again after administration of levodopa 200 mg.

Recordings

Subjects were supine and recorded at rest and/or while they tonically extended the wrist contralateral to the ME with which activity was recorded. EEG was recorded via bipolar Ag–AgCl electrodes (9 mm diameter). CzFz was the only available EEG electrode in all but four patients, as a result of limited scalp access due to surgical dressing and/or limited numbers of recording channels. Deep brain activity was recorded from the adjacent four contacts of each ME (0–1, 1–2, 2–3). EEG and LPs were filtered at 1–300 Hz and amplified (×100–500 000). Signals were sampled at 1 kHz, and recorded and monitored online. Amplification, filtering and recording were performed using the Schwartzer 34 amplifier system (Schwartzer GmbH, Medical Diagnostic Equipment, Munich, Germany) and Brainlab software (OSG bvba, Rumst, Belgium) at the Academic Medical Centre, Amsterdam. Signals were amplified and filtered using a custom-made, 9 V battery-operated portable amplifier, and recorded through an A-D card (PCM-DAS16S; ComputerBoards, Mass., USA) onto a portable computer using a custom written program at the CTO 'A. Alesini' Hospital, Rome. Subsequent analyses were performed using Spike 2 (Cambridge Electronic Design, Cambridge, UK).

Analysis

Our hypothesis required the demonstration of coherence and phase between cortex and basal ganglia in given frequency bands. Tonic contraction data durations were relatively short compared with rest (less than one-quarter of the total trial duration). Since fast Fourier analysis was the basic technique for estimation of spectral power, coherence and phase, optimization of estimates was achieved through a combination of rest and tonic activity. This is justified since acceptance of the hypothesis depends upon the demonstration

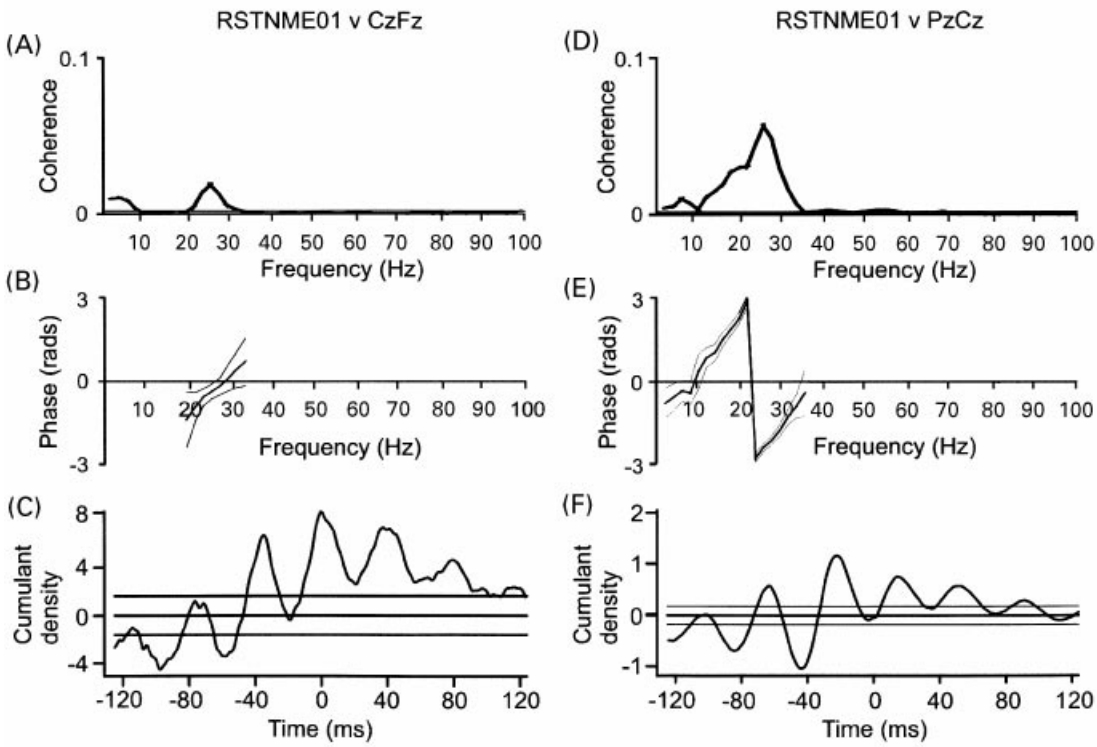

Fig. 2 Coherence and phase spectra and cumulant density estimates between the right (R) STNME01 and midline EEG activity in Case 4 on her usual anti-parkinsonian medication. (**A**–**C**) Results for STNME01 LP versus CzFz EEG. (**D**–**F**) results for STNME01 LP versus PzCz. Note that coherence at 20–30 Hz is seen with both scalp electrodes, but that over 10–20 Hz it is only seen with the posterior midline channel. EEG led STNME LP by 20–30 ms. The cumulant density estimates suggest polarity reversal about Cz for the activity with a period of ~40 ms, implying that the cortical activity coupled with the STNME LPs at 25 Hz arises in the area of Cz. The horizontal lines in the coherence spectra and cumulant density estimates and the thin lines in the phase spectra are the 95% CL (1499 blocks have been averaged).

of significant levels of coherent activity in given bands (not absolute levels) and, similarly, the examination of the relationship of phases between bands more than absolute phase determination. The EEG, denoted by subscript *x*, and LP, denoted by subscript *y*, were assumed to be realizations of stationary zero mean time series. The principal statistical tool used for data analysis in this study was the discrete Fourier transform and parameters derived from it, all of which were estimated by dividing the records into a number of disjointed sections of equal duration, and estimating spectra by averaging across these discrete sections (Halliday *et al*., 1995). In the frequency domain, estimates of the autospectrum of the EEG, $f_{xx}(\lambda)$, and LP, $f_{yy}(\lambda)$, were constructed, along with estimates of coherence, $|R_{xy}(\lambda)|^2$. Timing information between the EEG and LP signals was calculated from the phase spectrum $f_{xy}(\lambda)$, defined as the argument of the cross spectrum: $f_{xy}(\lambda) = \arg\{f_{xy}(\lambda)\}$. In the time domain, the cumulant density function, $q_{xy}(u)$, with LP as reference, was estimated from the cross spectrum, $f_{xy}(\lambda)$, via an inverse Fourier transform. Confidence limits (CL) for all parameters were estimated [for further details see Halliday *et al*. (1995)]. To compare coherences by ANOVA (analysis of variance), the variance of the modulus of the coherency (given by the square root of the coherence) was normalized using a Fisher transform. The variance of spectral power estimates was stabilized by logarithmic transformation. No corrections for non-sphericity were required in the ANOVAs.

When determining the cortical topography of coherence between EEG and STNME, data were down-sampled to 200 Hz and segment lengths of 256 points were used, giving a frequency resolution of 0.78 Hz (except in Fig. 1, in which segment length was 128 points and resolution 1.56 Hz). A mean of 280 segments (range 122–410) was averaged. Phase was only analysed over those frequencies showing significant coherence between STN/GPi and cortex. A segment length of 512 points (resolution 1.95 Hz with a sampling rate of 1 kHz) gave the best compromise between frequency resolution and variance in the phase estimate. For phase estimates, a mean of 976 segments (range 451–2044) was averaged. The constant time lag between two signals was calculated from the slope of the phase estimate after a line had been fitted by linear regression. The time lag was only calculated from the gradient if the number of contiguous data points included in the segment was five or more, and a linear relationship accounted for (r^2) $\geqslant$71% of the variance ($P < 0.05$). The phase between STNME LP and CzFz EEG did not meet these criteria in six patients in whom only CzFz was available, and these were not included in the present paper.

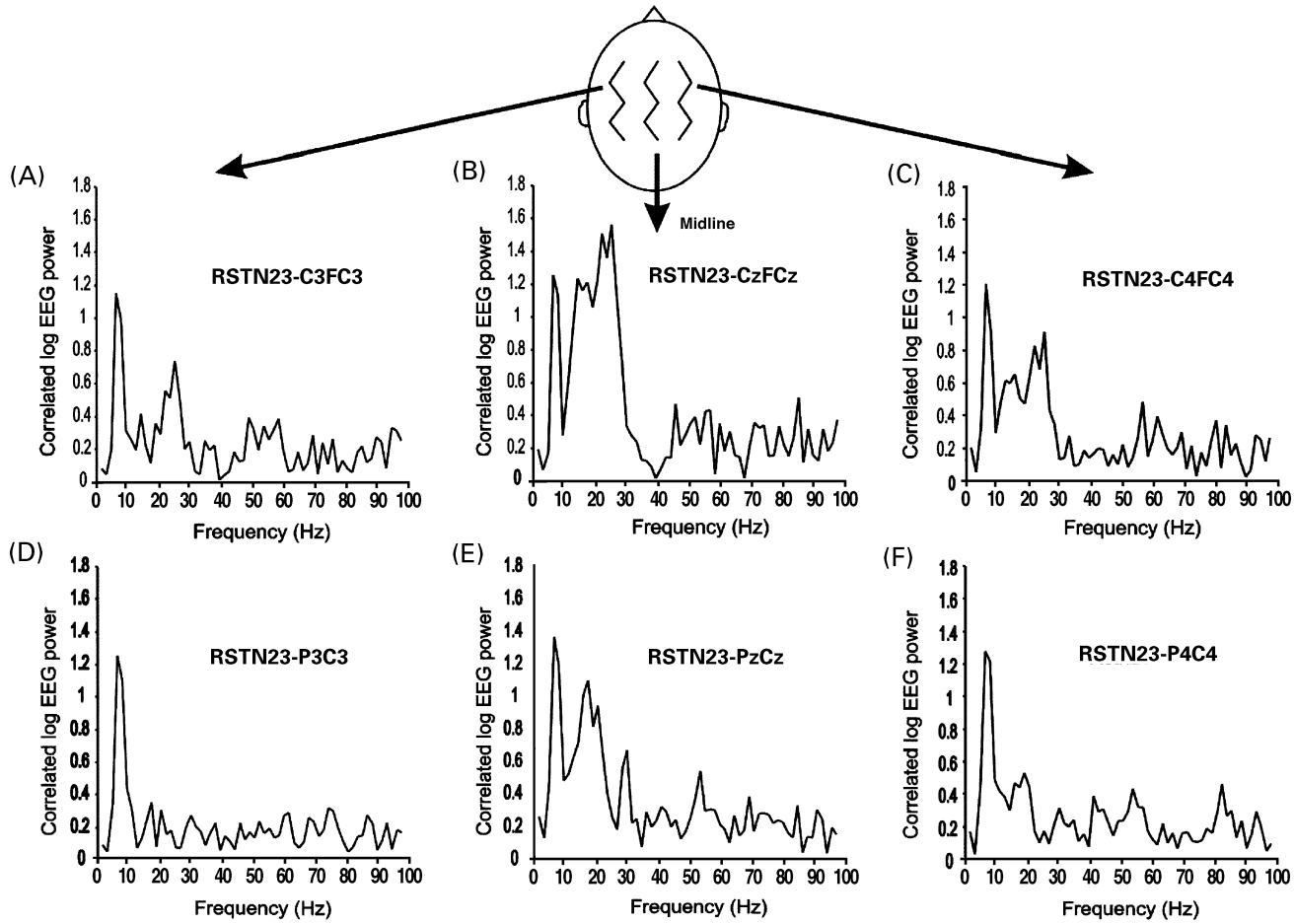

Fig. 3 The log-transformed EEG power at each bipolar electrode correlated in a linear fashion with the signal from right (R) STNME23 in Case 1 on his usual anti-parkinsonian medication. Coupling is strongest over the midline. The same data have been analysed as in Fig. 1.

Results

Patients were divided into two groups. In Group 1 (Cases 1–4), an EEG was recorded using multiple electrodes, but recordings were only made during treatment with routine anti-parkinsonian medication. In Group 2 (Cases 5–8) only CzFz was available, and recordings were performed after overnight withdrawal of medication, and again after levodopa in each case. The first group permitted an analysis of the topography of those cortical areas coupled to STNME activity, while the second group allowed temporal differences between cortex and STNME and, in Cases 7 and 8, GPiME to be compared at different frequencies in the same subjects.

Dependence of coherence between STN and cortex on cortical leads (Cases 1–4)

Coherence between EEG and STNME LP was apparent in three major frequency bands: 2–10 Hz, 10–30 Hz and 70–85 Hz. The presence or absence of coherence in these frequency bands is summarized for each patient in Table 1, and Fig. 1 shows a representative example of the cortical topography of STNME EEG coherence in Case 1.

Coherence at 2–10 Hz was fairly evenly distributed over the midline and lateral cortical areas compared with that in the 10–30 Hz band. Coherence at these low frequencies between activity in the human globus pallidus and tremor has been reported previously (Hurtado *et al*., 1999), while the presence of tremor-related neuronal discharge in the human STN is well recognized (Hutchinson *et al*., 1998; Bejjani *et al*., 2000). The coherence at frequencies >10 Hz was greater over midline cortical areas than ipsilaterally, and much greater than contralaterally in all four patients (Fig. 1). Topographic differences between transformed coherences in the 2–10 Hz and 10–30 Hz bands across all four patients were confirmed by a two-way ANOVA with area (midline, ipsilateral and contralateral to the ME) and frequency (2–10 Hz and 10–30 Hz) as factors. There was no main effect for frequency, but there was a significant main effect for area (F = 8.757, P = 0.017) and an interaction between area and frequency (F = 7.944, P = 0.021). Post hoc paired t-tests confirmed that the transformed coherence in the 10–30 Hz band was greater in the midline than contralaterally (P = 0.030) or ipsilaterally (P = 0.026) and that transformed coherence ipsilateral to the ME in the 2–10 Hz band was greater than that contralaterally (P = 0.039). There were no

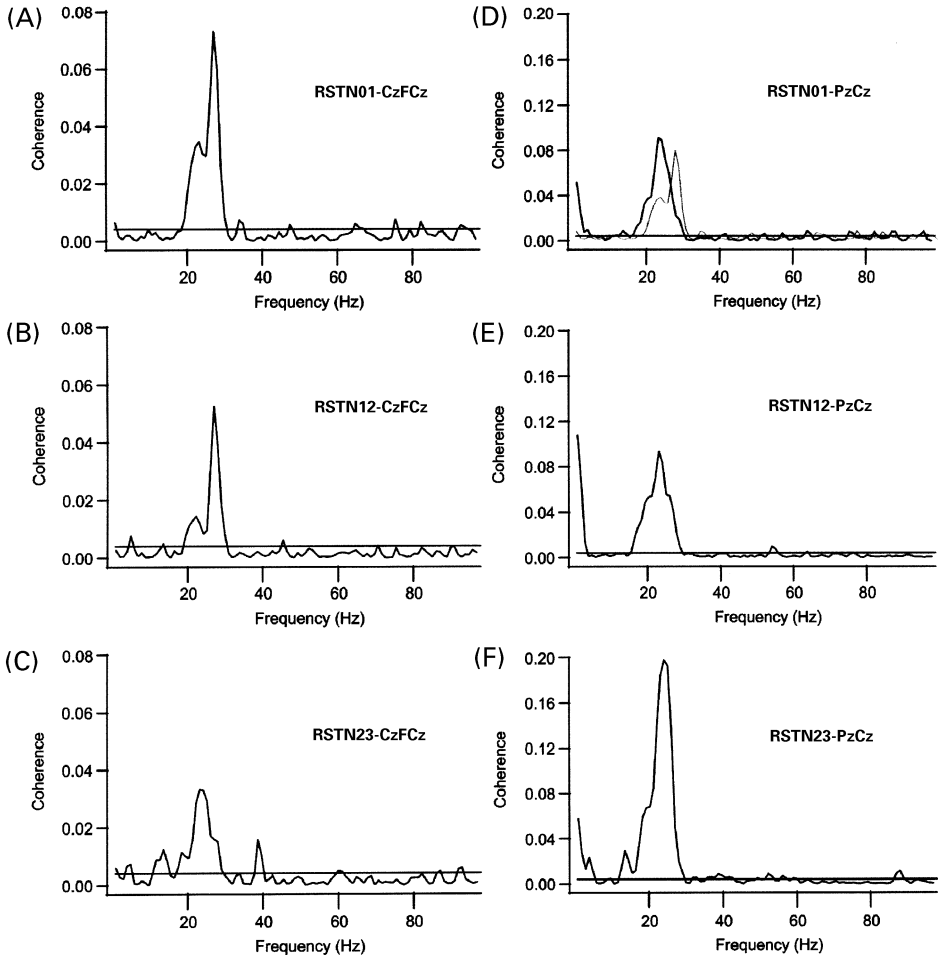

Fig. 4 Coherence spectra between right (R) STNME and CzFCz (**A**–**C**) and PzCz (**D**–**F**) in Case 4 on her usual anti-parkinsonian medication. Note that peak coherence between STNME and PzCz had a slightly lower frequency (the spectrum from **A** has been superimposed in grey on **D** for a comparison of frequencies) and a different distribution around the STN (287 blocks have been averaged).

significant differences between transformed coherences over the different cortical areas in the 2–10 Hz band otherwise.

The activity at 10–30 Hz could be subdivided into two further bands. Activity at the lower frequency was proportionately greater in the posterior midline bipolar lead than in the anterior midline (compare Figs 1B, 2A, 3B and 4A with Figs 1E, 2D, 3E and 4D, respectively), although differences were not confirmed by an ANOVA with area (anterior midline and posterior midline) and frequency (15–22 Hz and 23–30 Hz) as factors, perhaps due to the small number of subjects. Coherence at 10–30 Hz was evident in all four cases. Coherence between 70 and 85 Hz was only present in one case with multiple EEG recording sites (Case 2). In this patient it was only seen following treatment with levodopa and was only recorded between STNME LP and CzFz, perhaps because the four patients were studied on their usual medication rather than at the time of peak anti-parkinsonian effects of levodopa 200 mg given after overnight drug withdrawal (as in Cases 5–8).

In summary, EEG-STNME coherence was greatest over midline cortical areas in the 10–30 Hz band. However, coherence analysis may have its drawbacks when determining the topography of cortical areas coupled to STN activity. These are problems of volume conduction and, most importantly, non-linear data contamination (see, for example, Florian *et al*., 1998). The largest source of non-linearly coupled activity over the frequencies of interest is EMG artefact. As coherence is a normalized measure, greater contamination of EEG signals by EMG over lateral compared with the midline channels might lead to spuriously low estimates of coupling with STN over lateral cortical areas.

The absolute magnitude of EEG power linearly correlated with the STNME signal can be estimated by multiplying the autospectra by the coherence spectra (see, for example, Mima *et al*., 2000). The log-transformed EEG power at each bipolar electrode, linearly correlated with the STNME signal, was therefore calculated. Figure 3 shows the distribution in Case 1, and it is noteworthy that the distribution was similar to that

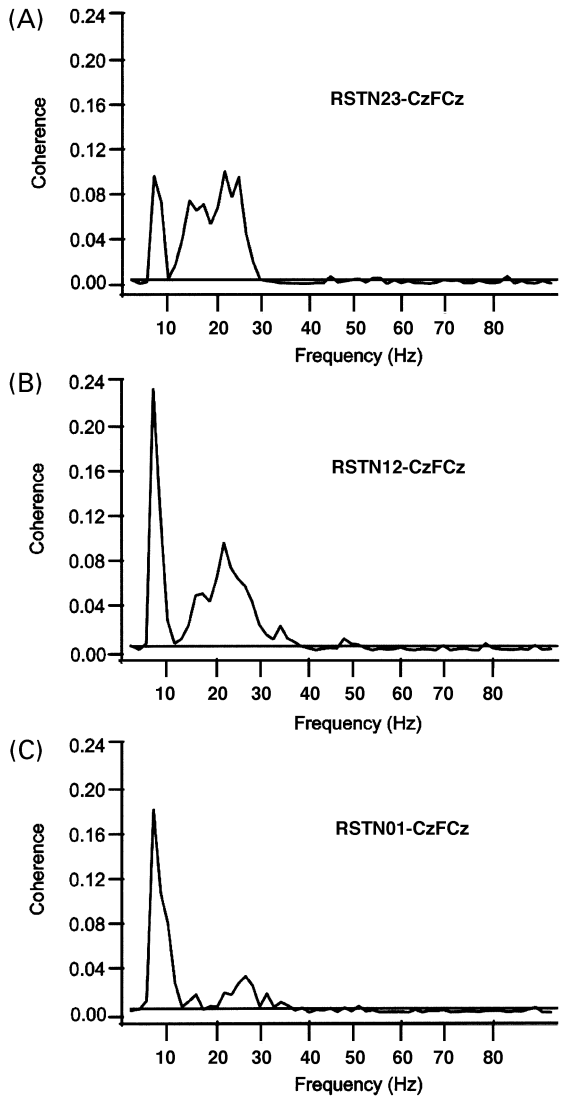

Fig. 5 Coherence spectra between right (R) STNME contacts and CzFCz in Case 1 on his usual anti-parkinsonian medication. Note that tremor-related coherence at frequencies below 10 Hz was greatest at leads 01 and 12, while that at 10–30 Hz was greatest at leads 12 and 23 (300 blocks have been averaged).

seen in Fig. 1. In particular, coupling at 10–30 Hz remained strongest over the midline. The importance of the midline electrodes was further supported by the identification of one instance of clear polarity reversal at Cz in cumulant density estimates (Fig. 2). Polarity reversal involved activity with a period of 40 ms, consistent with a frequency of 25 Hz.

It was noteworthy that the EEG-STNME coherence at 10–30 Hz and that at 2–10 Hz was greatest in different STNME leads in three out of the four patients, as illustrated in Fig. 5. In addition, within the 10–30 Hz frequency band, coherence between CzFz and STN and between PzCz and STN was greatest at different STNME leads in two patients, as shown in Fig. 4. The pattern of the log-transformed LP power at each bipolar STN electrode linearly correlated with EEG (not shown) was similar to that seen in Figs 4 and 5, so that variations in coherence were unlikely to be due to different degrees of non-linear contamination. These observations suggest that different oscillatory activities could have slightly different origins within STN and the surrounding fields. Nevertheless, we were unable to find any convincing examples of polarity reversal at different STNME contacts for any of the different oscillatory activities, perhaps due to the small size of STN relative to the distance between electrode contacts (Hutchinson *et al*., 1998; Ashby *et al*., 1999). The latter means that differences in the distribution of oscillatory activities within the STN cannot be seen as different sites of polarity reversal (as this would require at least two ME contacts within the STN), although they might lead to variations in the coherence between contact pairs and EEG.

Phase relationships and effects of levodopa (Cases 5–8)

Phase relationships were determined in the four patients in Group 2. A representative example of the autospectra, coherence and phase spectra from data recorded on and off levodopa in a patient with only a single STNME (Case 5) is illustrated in Fig. 6. Strong coherence between STNME and CzFz is evident at 70–85 Hz, but only after treatment with levodopa.

Coherence at 70–85 Hz was limited to the treated 'on' state in all four patients and was only evident at a maximum of two bipolar pairs of contiguous contacts. The time differences between STN and EEG activity calculated from phase spectra are summarized for all subjects in Fig. 7. Both on and off dopaminergic therapy, activity at CzFz led the activity picked up by the STNME by 26.1 $\pm$ 5.4 ms (mean $\pm$ standard error of the mean) at frequencies <30 Hz. In contrast, activity at the STNME led that at CzFz by 17.3 $\pm$ 4.3 ms over the 70–85 Hz band. Two patients in this group also had a unilateral GPiME implanted at the same time as the STNME. The phase relationship between EEG and GPiME LP was similar to that found with the STNME. Activity at CzFz led the GPiME LP by 21 ms (Case 7) and 15 ms (Case 8) at frequencies <40 Hz. However, in the one patient in whom phase could be determined over the 70–85 Hz band, activity at the GPiME led CzFz EEG by 4 ms. Figure 8 compares the phase and coherence spectra on and off treatment between CzFz EEG and STNME LP, and CzFz EEG and GPiME LP in Case 8. The spectra are derived from simultaneous recordings from the two sites and their general pattern is similar.

In summary, autospectra, coherence and phase spectra were similar in Cases 5–8, with relatively little difference between STN and GPi. The biggest differences were seen within the same subject, according to treatment state. Coherence between STN and EEG, and GPi and EEG at high frequency was seen only after treatment with levodopa.

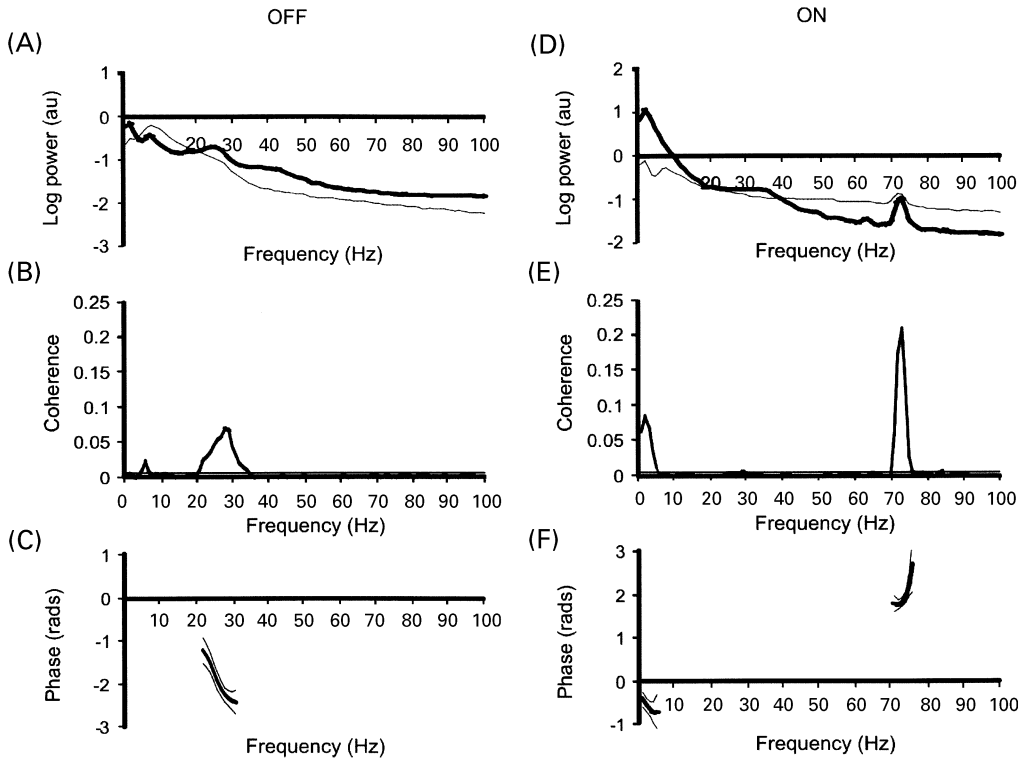

Fig. 6 Power, coherence and phase spectra for CzFz and left (L) STNME23 in Case 5. (**A**–**C**) and (**D**–**F**) are the results after withdrawal (OFF) and reinstitution of treatment (ON) with levodopa, respectively. The bold and thin lines in the power spectra represent the STNME LP and CzFz EEG, respectively. Note the shift in coherence to higher frequencies and the reversal of the phase slope after treatment with levodopa (918 blocks have been averaged off and on treatment).

Discussion

The data presented here support the hypothesis that activity in circuits linking the human basal ganglia and cerebral cortex have a complex organization in the frequency domain, with multiple modes of oscillation. We provide evidence that different oscillatory activities differ in their cortical topography, and in their distribution within the STN and surrounding fields. Importantly, different oscillatory activities may also be characterized by their phase relationship with cortex. Oscillations are divided into those <30 Hz in which, overall, cortex drives the basal ganglia, in agreement with our previous findings (Marsden *et al*., 2001), and those at higher frequency in which STN drives cortex. Fast activity (70–85 Hz) was only recorded following treatment with levodopa, consistent with previous findings (Brown *et al*., 2001).

These various observations argue in favour of multiple, functionally heterogeneous oscillatory activities linking the human basal ganglia and cerebral cortex. This is in line with current views of multiple anatomically segregated circuits linking basal ganglia and cortex (Alexander *et al*., 1990), although this is not to say that specific oscillatory activities can be associated with specific anatomical pathways. The notion that the human basal ganglia may consist of multiple independent oscillating circuits was first suggested by Hurtado *et al*. based on the dynamics of tremor-related oscillations in the globus pallidus (Hurtado *et al*., 1999). The present work builds on this, extending the frequency range of oscillatory circuits and demonstrating that these circuits extend to involve STN and cortex. Nevertheless, before

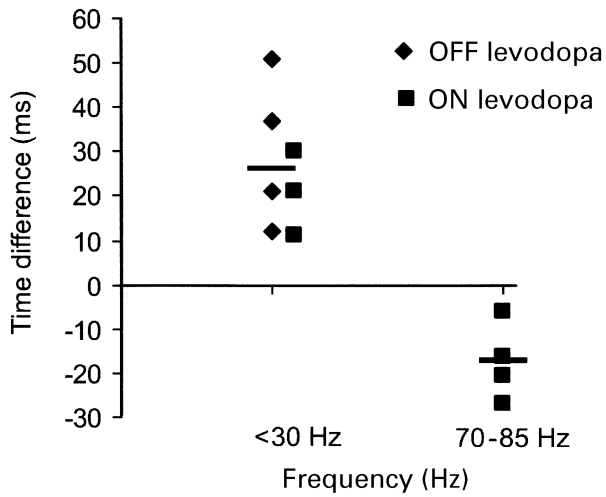

Fig. 7 Time differences between STNME LP and CzFCz. Positive latencies indicate that the EEG phase led the STNME LP. For frequencies <30 Hz, EEG led STNME LP by a mean (indicated by a horizontal bar) of 26.1 ms (95% CL 12.9–39.3 ms), but over the 70–85 Hz band STNME LP led EEG by a mean of 17.3 ms (CL, confidence limit, 3.5–30.9 ms).

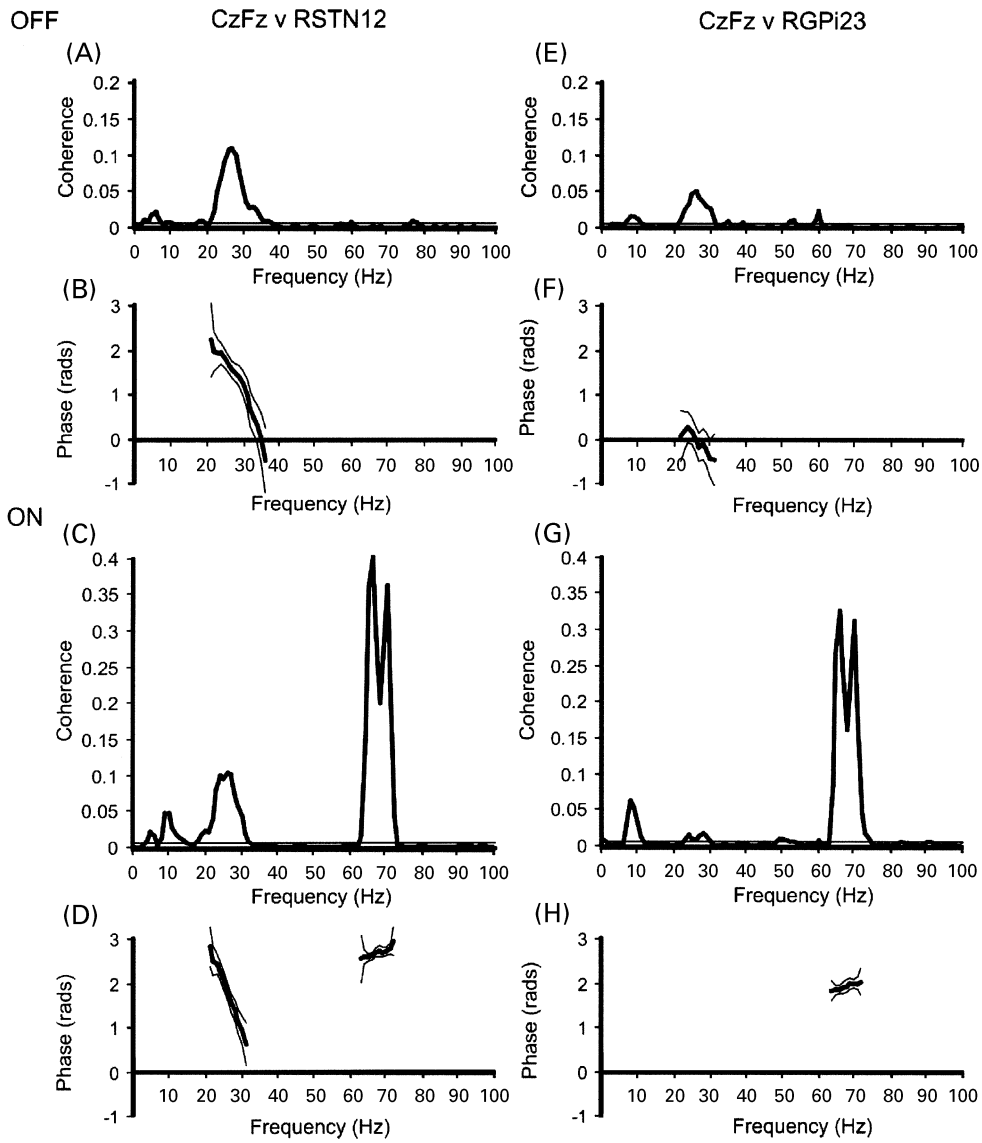

Fig. 8 Coherence and phase spectra between CzFCz and right (R) STNME (**A**–**D**) or right GPiME (**E**–**H**) in Case 8. **A**, **B**, **E** and **F**, and **C**, **D**, **G** and **H** are the results after withdrawal (OFF) and reinstitution of treatment (ON) with levodopa, respectively. Note the shift in coherence to higher frequencies, and the reversal of the phase slope after treatment with levodopa. The pattern is similar for STN and GPi (451 blocks have been averaged off and on treatment).

discussing our results further, we should bear in mind one of the major limitations of human recordings, that placement of depth MEs within their intended targets is presumptive and not backed up by histological confirmation as in animal studies.

The temporal differences with which cortical activity led or lagged behind that in STN were similar, around 20 ms, regardless of the overall direction of information flow and frequency band. Where STN drives cortex the likely path, based on anatomical considerations (Parent and Hazrati, 1995), is via GPi/substantia nigra pars reticulata and thalamus, and a delay of 20 ms or so seems reasonable. Where cortex drives STN this could be achieved either directly through the large cortico-subthalmic projection, or indirectly via the putamen/globus pallidus externa (Parent and Hazrati, 1995). A delay of ~20 ms would seem to favour the latter, and it is noteworthy that similar delays were seen between cortex and GPi, where pathways are, necessarily so, indirect. In contrast, stimuli applied within the motor cortex of the monkey facilitate STN neurones with a mean latency of 5.8 ms (Nambu *et al*., 2000) and frontal cortical potentials may be elicited with a latency of 5–8 ms after probable

antidromic activation of the direct cortico-subthalamic pathways in humans (Ashby *et al*., 2001).

The central role of midline cortical motor areas

We were only able to analyse scalp EEG from up to nine sites. Nevertheless, coherence was greatest over midline cortical areas and there was one instance of polarity reversal around Cz. These results suggest that functional connections are particularly strong between STN and the midline cortical areas, particularly the supplementary motor area (SMA), underlying Cz. This is consistent with other data indicating a central role for SMA in motor loops involving the basal ganglia and cortex. Activity in SMA is a major contributor to the Bereitschafts-potential that precedes self-generated movements (Kornhuber and Deecke, 1965; Shibasaki *et al*., 1980; Deecke, 1987), and this potential is reduced in Parkinson's disease (Deecke *et al*., 1977; Shibasaki *et al*., 1978; Dick *et al*., 1987, 1989; Cunnington *et al*., 1995; Jahanshahi *et al*., 1995). Imaging studies confirm impaired activation of SMA during some movements in untreated Parkinson's disease (Playford *et al*., 1992; Rascol *et al*., 1992; Jahanshahi *et al*., 1995; Limousin *et al*., 1997), which is reversible using the dopaminergic agonist apomorphine (Jenkins *et al*., 1992; Rascol *et al*., 1992). Our results suggest a net transmission of information from midline cortical motor areas to STN at frequencies <30 Hz, and transmission from STN back to these midline areas in the 70–85 Hz band.

In contrast, there was relatively little coherence at frequencies above 10 Hz over lateral electrodes covering the sensorimotor and premotor cortices, suggesting that oscillatory coupling between STN and these cortical areas is not as important as that with midline areas such as SMA. This is consistent with imaging data suggesting that activation of the sensorimotor and premotor cortices is relatively normal, or may even show a compensatory increase in Parkinson's disease (Playford *et al*., 1992; Jahanshahi *et al*., 1995; Samuel *et al*., 1997; Sabatini *et al*., 2000).

Roles of oscillatory activity

The role or roles of oscillatory neuronal behaviour in subcortico-cortical loops remains open to speculation. The coherence between STN/GPi and cortex at 2–10 Hz may be related to parkinsonian rest tremor (Volkmann *et al*., 1996; Hurtado *et al*., 1999), while Levy *et al*. have argued that oscillatory activity in the 20–30 Hz band, intrinsic to the STN, may also be related to pathological tremor (Levy *et al*., 2000). However, the presence of oscillatory STN LPs at 20–30 Hz and 70–85 Hz in parkinsonian patients without tremor (Brown *et al*., 2001) and in the GPi of patients with dystonia (personal observations) argues that these high frequency activities may be more fundamental in their significance. One possibility is that synchronous oscillations may act to temporally coordinate circuits to produce motor acts in a manner analogous to that posited in perceptual binding (Gray *et al*., 1989). The basal ganglia may be simultaneously involved in a myriad of tasks, which, even in just the motor sphere, include motor planning, sequencing, attentional changes, feedback processing and learning. The dynamic organization of activities in the frequency domain might provide a means for temporal coordination within and across different processing streams in the basal ganglia (Graybiel *et al*., 1994). However, if this is the case then this function must be achieved on a relatively small scale as the evidence suggests that oscillatory activities exhibit some degree of anatomical segregation.

An alternative but not necessarily mutually exclusive view is that the oscillations, particularly those <30 Hz, may represent some temporal aspect of movement. This has been suggested by Nicolelis *et al*. who observed 7–12 Hz oscillations between the sensorimotor cortex and the ventral posterior medial nucleus of the rat during active whisker exploration of the environment (Nicolelis *et al*., 1995). Interestingly the thalamic activity lagged behind cortical oscillations (Nicolelis *et al*., 1995), as seen at frequencies <30 Hz in the present study. Nicolelis *et al*. proposed that the oscillations were an internally generated temporal representation of exploratory movements in the sensorimotor domain (Nicolelis *et al*., 1995). Therefore it is possible that the coherent activities demonstrated here may provide a common mechanism for the temporal sampling of movement-related activities within the sensorimotor cortex and basal ganglia, as suggested within the sensorimotor cortex and cerebellar systems (Marsden *et al*., 2000). In the latter case, subcortico-cortical coupling occurs at frequencies <30 Hz and therefore involves the same frequency band as coupling between motor cortex and muscle (Marsden *et al*., 2000). One major advantage of this putative temporal framework is the potential for the systematic modulation of gain at different phases of the sampling cycle. As the period of the sampling cycle matches that of the rhythmic motor output (Conway *et al*., 1995; Salenius *et al*., 1997; Brown *et al*., 1998; Halliday *et al*., 1998; Mima and Hallett, 1999), afferent input can be weighted according to the phase of motor output. In this hypothetical mechanism the sensorimotor cortex would be continuously digitising activity in the basal ganglia and cerebellar systems, explaining why subcortico-cortical coherence is present at rest as well as during activity. These oscillations may then interact with and entrain afferent input routed through the basal ganglia and cerebellum during activity.

Regardless of whether subcortico–cortical synchronization is primarily physiological or a pathological consequence of Parkinson's disease, it is likely to be important in functional terms. Synchronization increases post-synaptic efficacy at subsequent projection targets, while non-linearities in the frequency–current relationship of basal ganglia neurones may increase the saliency of inputs in particular frequency bands (Bevan and Wilson, 1999). The present findings are important in suggesting that there may be some frequency selectivity of coupling according to the cortical and basal ganglia fields

involved. Nevertheless, coupling is likely to be dynamic, changing with movement and dopaminergic state (Brown *et al*., 2001). The latter, in particular, seems to dictate the degree to which oscillatory subthalamo-cortical coupling is two-way and not just corticofugal. Further investigation is required to identify whether different oscillatory patterns have different behavioural correlates, and whether the pattern of LP oscillation recorded during functional neurosurgery might help predict outcome.

Acknowledgements

We are grateful to Professor D. Thomas and Dr G. Jacopino who performed the surgery in Cases 5 and 6, respectively, and Mr D. Buckwell, Dr D. Halliday and Dr J. Ogden for computer programs. This work was supported by the Medical Research Council and GlaxoSmithKline.

References

Alexander GE, Crutcher MD, DeLong MR. Basal ganglia-thalamocortical circuits: parallel substrates for motor, oculomotor, 'prefrontal' and 'limbic' functions. [Review]. Prog Brain Res 1990; 85: 119–46.

Ashby P, Kim YJ, Kumar R, Lang AE, Lozano AM. Neurophysiological effects of stimulation through electrodes in the human subthalamic nucleus. Brain 1999; 122: 1919–31.

Ashby P, Paradiso G, Saint-Cyr JA, Chen R, Lang AE, Lozano AM. Potentials recorded at the scalp by stimulation near the human subthalamic nucleus. Clin Neurophysiol 2001; 112: 431–7.

Bejjani BP, Dormont D, Pidoux B, Yelnik J, Damier P, Arnulf I, et al. Bilateral subthalamic stimulation for Parkinson's disease by using three-dimensional stereotactic magnetic resonance imaging and electrophysiological guidance. J Neurosurg 2000; 92: 615–25.

Bevan MD, Wilson CJ. Mechanisms underlying spontaneous oscillation and rhythmic firing in rat subthalamic neurons. J Neurosci 1999; 19: 7617–28.

Brown P, Salenius S, Rothwell JC, Hari R. The cortical correlate of the Piper rhythm in humans. J Neurophysiol 1998; 80: 2911–7.

Brown P, Oliviero A, Mazzone P, Insola A, Tonali P, Di Lazzaro V. Dopamine dependency of oscillations between subthalamic nucleus and pallidum in Parkinson's disease. J Neurosci 2001; 21: 1033–8.

Conway BA, Halliday DM, Farmer SF, Shahani U, Maas P, Weir AL, et al. Synchronization between motor cortex and spinal motoneuronal pool during the performance of a maintained motor task in man. J Physiol (Lond) 1995; 489: 917–24.

Cunnington R, Iansek R, Bradshaw JL, Philips JG. Movement-related potentials in Parkinson's disease. Presence and predictability of temporal and spatial cues. Brain 1995; 118: 935–50.

Deecke L, Englitz HG, Kornhuber HH, Schmitt G. Cerebral potentials preceding voluntary movement in patients with bilateral or unilateral Parkinson akinesia. Prog Clin Neurophysiol 1977; 1: 151–63.

Deecke L, Lang W, Heller HJ, Hufnagl M, Kornhuber HH. Bereitschaftspotential in patients with unilateral lesions of the supplementary motor area. J Neurol Neurosurg Psychiatry 1987; 50: 1430–4.

Dick JP, Cantello R, Buruma O, Gioux M, Benecke R, Day BL, et al. The Bereitschaftspotential, L-DOPA and Parkinson's disease. Electroencephalogr Clin Neurophysiol 1987; 66: 263–74.

Dick JP, Rothwell JC, Day BL, Cantello R, Buruma O, Gioux M, et al. The Bereitschaftspotential is abnormal in Parkinson's disease. Brain 1989; 112: 233–44.

Florian G, Andrew C, Pfurtscheller G. Do changes in coherence always reflect changes in functional coupling? Electroencephalogr Clin Neurophysiol 1998; 106: 87–91.

Gray CM, Konig P, Engel AK, Singer W. Oscillatory responses in cat visual cortex exhibit inter-columnar synchronization which reflects global stimulus properties. Nature 1989; 338: 334–7.

Graybiel AM, Aosaki T, Flaherty AW, Kimura M. The basal ganglia and adaptive motor control. [Review]. Science 1994; 265: 1826–31.

Halliday DM, Rosenberg JR, Amjad AM, Breeze P, Conway BA, Farmer SF. A framework for the analysis of mixed time series/point process data—theory and application to the study of physiological tremor, single motor unit discharges and electromyograms. Prog Biophys Mol Biol 1995; 64: 237–78.

Halliday DM, Conway BA, Farmer SF, Rosenberg JR. Using electroencephalography to study functional coupling between cortical activity and electromyograms during voluntary contractions in humans. [Review]. Neurosci Lett 1998; 241: 5–8.

Hurtado JM, Gray CM, Tamas LB, Sigvardt KA. Dynamics of tremor-related oscillations in the human globus pallidus: a single case study. Proc Natl Acad Sci USA 1999; 96: 1674–9.

Hutchinson WD, Allan RJ, Opitz H, Levy R, Dostrovsky JO, Lang AE, et al. Neurophysiological identification of the subthalamic nucleus in surgery for Parkinson's disease. Ann Neurol 1998; 44: 622–8.

Jahanshahi M, Jenkins IH, Brown RG, Marsden CD, Passingham RE, Brooks DJ. Self-initiated versus externally triggered movements. I. An investigation using measurement of regional cerebral blood flow with PET and movement-related potentials in normal and Parkinson's disease subjects. Brain 1995; 118: 913–33.

Jenkins IH, Fernandez W, Playford ED Lees AJ, Frackowiak RS, Passingham RE, et al. Impaired activation of the supplementary motor area in Parkinson's disease is reversed when akinesia is treated with apomorphine. Ann Neurol 1992; 32: 749–57.

Kornhuber HH, Deecke L. Hirnpotentialanderungen bei Willkurbewegungen und passiven Bewegungen des Menschen: Bereitschaftspotential und reafferente Potentiale. Pfluger Arch Ges Physiol 1965; 284: 1–17.

Levy R, Hutchison WD, Lozano AM, Dostrovsky JO. High-frequency synchronization of neuronal activity in the subthalamic nucleus of parkinsonian patients with limb tremor. J Neurosci 2000; 20: 7766–75.

Limousin P, Pollak P, Bennazzouz A, Hoffmann D, Le Bas JF,

Brouseolle E, et al. Effect of parkinsonian signs and symptoms of bilateral subthalamic nucleus stimulation. Lancet 1995; 345: 91–5.

Limousin P, Greene J, Pollak P, Rothwell J, Benabid AL, Frackowiak R. Changes in cerebral activity pattern due to subthalamic nucleus or internal pallidum stimulation in Parkinson's disease. Ann Neurol 1997; 42: 283–91.

Marsden JF, Ashby P, Limousin-Dowsey P, Rothwell JC, Brown P. Coherence between cerebellar thalamus, cortex and muscle in man. Cerebellar thalamus interactions. Brain 2000; 123: 1459–70.

Marsden JF, Limousin-Dowsey P, Ashby P, Pollak P, Brown P. Subthalamic nucleus, sensorimotor cortex and muscle interrelationships in Parkinson's disease. Brain 2001; 124: 378–88.

Mima T, Hallett M. Electroencephalographic analysis of cortico-muscular coherence: reference effect, volume conduction and generator mechanism. Clin Neurophysiol 1999; 110: 1892–9.

Mima T, Matsuoka T, Hallett M. Functional coupling of human right and left cortical motor areas demonstrated with partial coherence analysis. Neurosci Lett 2000; 287: 93–6.

Nambu A, Tokuno H, Hamada I, Kita H, Imanishi M, Akazawa T, et al. Excitatory cortical inputs to pallidal neurons via the subthalamic nucleus in the monkey. J Neurophysiol 2000; 84: 289–300.

Nicolelis MA, Baccala LA, Lin RC, Chapin JK. Sensorimotor encoding by synchronous neural ensemble activity at multiple levels of the somatosensory system. Science 1995; 268: 1353–8.

Parent A, Hazrati L-N. Functional anatomy of the basal ganglia. II. The place of the subthalamic nucleus and external pallidum in basal ganglia circuitry. [Review]. Brain Res Brain Res Rev 1995; 20: 128–54.

Playford ED, Jenkins IH, Passingham RE, Nutt J, Frackowiak RS, Brooks DJ. Impaired mesial frontal and putamen activation in Parkinson's disease: a positron emission tomography study. Ann Neurol 1992; 32: 151–61.

Rascol O, Sabatini U, Chollet F, Celsis P, Montastruc JL, Marc-Vergnes J-P, et al. Supplementary and primary sensory motor area activity in Parkinson's disease. Arch Neurol 1992; 49: 144–8.

Sabatini U, Boulanouar K, Fabre N, Martin F, Carel C, Colonnese C, et al. Cortical motor reorganization in akinetic patients with Parkinson's disease: a functional MRI study. Brain 2000; 123: 394–403.

Salenius S, Portin K, Kajola M, Salmelin R, Hari R. Cortical control of human motoneuron firing during isometric contraction. J Neurophysiol 1997; 77: 3401–5.

Samuel M, Ceballos-Baumann AO, Blin J, Uema T, Boecker H, Passingham RE, et al. Evidence for lateral premotor and parietal overactivity in Parkinson's disease during sequential and bimanual movements. A PET study. Brain 1997; 120: 963–76.

Shibasaki H, Shima F, Kuroiwa Y. Clinical studies of the movement-related cortical potential (MP) and the relationship between the dentatorubrothalamic pathway and readiness potential (RP). J Neurol 1978; 219: 15–25.

Shibasaki H, Barrett G, Halliday E, Halliday AM. Components of the movement-related cortical potential and their scalp topography. Electroencephalogr Clin Neurophysiol 1980; 49: 213–26.

Siegfried J, Lippitz B. Bilateral chronic electrostimulation of ventroposterolateral pallidum: a new therapeutic approach to alleviating all parkinsonian symptoms. Neurosurgery 1994; 35: 1126–30.

Starr PA, Vitek JL, Bakay RA. Ablative surgery and deep brain stimulation for Parkinson's disease. [Review]. Neurosurgery 1998; 43: 989–1015.

Volkmann J, Joliot M, Mogilner A, Ioannides AA, Lado F, Fazzini E, et al. Central motor loop oscillations in parkinsonian resting tremor revealed by magnetoencephalography. Neurology 1996; 46: 1359–70.

Volkmann J, Sturm V, Weiss P, Kappler J, Voges J, Koulousakis A, et al. Bilateral high-frequency stimulation of the internal globus pallidus in advanced Parkinson's disease. Ann Neurol 1998; 44: 951–61.

Received September 17, 2001. Revised January 21, 2002.
Accepted January 29, 2002